RELATIVE BUNCH LENGTH MONITOR FOR THE LINAC COHERENT LIGHT SOURCE (LCLS) USING COHERENT EDGE RADIATION*

H. Loos[†], T. Borden, P. Emma, J. Frisch, J. Wu, SLAC, Menlo Park, CA 94025, USA

Abstract

The ultra-short bunches of the electron beam for LCLS are generated in two 4-dipole bunch compressors located at energies of 250 MeV and 4.3 GeV. Although an absolute measurement of the bunch length can be done by using a transverse deflecting cavity in an interceptive mode, a non-interceptive single shot method is needed as a relative measurement of the bunch length used in the continuous feedback for beam energy and peak current. We report on the design and implementation of two monitors measuring the integrated power of coherent edge radiation from the last dipole in each chicane.

INTRODUCTION

The high peak current of several kA of the LCLS electron beam required to saturate the FEL process is generated in two subsequent chicane bunch compressors at 0.25 and 4.3 GeV. To enable stable operation of the FEL, the peak current has to be maintained within 10% of its nominal value. Previous studies [1] have shown that this can be accomplished in a feedback by measuring non-invasively the relative shot to shot bunch length after each bunch compressor with 5% resolution. This measurement of the bunch length can be relative because it can be calibrated against an absolute, but invasive measurement which is available with a transverse deflecting cavity. The electron beam and chicane dipole parameters are listed in Table 1.

Table 1: Bunch length monitor requirements. The numbers in the table correspond to two different configurations with 0.2 and 1 nC of bunch charge.

Parameter	Unit	BC1	BC2
Electron beam energy	GeV	0.25	4.3
Charge range	nC	0.2 - 1	0.2 - 1
Nominal rms bunch length	μm	60 - 200	8 - 20
Bunch length range	μm	25 - 360	4 - 40
Length of dipole magnet	m	0.2	0.5
Bend angle of magnet	mrad	90 - 87	30 - 35
Free space after magnet	m	0.3	0.6

The use of the coherent synchrotron radiation from the last bend magnet in each chicane has previously been investigated [2]. Here we report on the simulation and design of the bunch length monitor presently being installed, which is based on the detection of coherent edge radiation [3] integrated within a certain spectral range.

The coherent radiation spectrum emitted from an electron bunch is generally the product of the single electron emission spectrum which depends on the radiation process and the bunch form factor which is the Fourier transform of the longitudinal charge distribution. When expanding the form factor for small wave numbers, it is evident that the form factor depends only on the rms bunch length.

$$f(k) = \left| \int dz e^{ikz} S(z) \right|^2 = 1 - k^2\sigma_{\mathrm{rms}}^2 + O(k^4) \quad (1)$$

The useful spectral range to determine the rms bunch length is then for $\lambda > 2\pi\sigma_{\mathrm{rms}}$, where the form factor does not depend on the specific details of the charge distribution. The form factor is shown in Fig. 1 for the nominal bunch length after bunch compressor 1 and 2. The spectral range for bunch length monitor 1 (BL1) is then $10 - 1$ mm and $1 - 0.1$ mm for BL2.
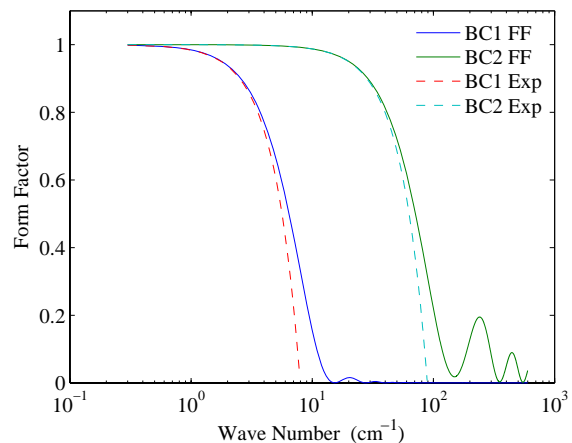

Figure 1: Electron bunch form factor for the 1 nC configuration. The solid lines represent the form factor for the simulated charge distribution and the dashed lines show the expansion for small frequencies using the rms bunch length.

EDGE RADIATION SIMULATION

The principal layout to detect coherent radiation from a dipole magnet is shown in Fig. 2. Synchrotron radiation is emitted from the bend path in the dipole and edge radiation from the sudden change in magnetic field at the entrance (not shown) and exit face of the magnet. The radiation is

06 Instrumentation, Controls, Feedback & Operational Aspects

T03 Beam Diagnostics and Instrumentation

coupled into a detector by means of a mirror with a hole large enough to not obstruct the electron beam and focusing optics to collimate the light from the magnet on the detector. The mirror itself is also a source of diffraction radiation. The critical wavelength of the synchrotron radiation is orders of magnitude smaller than the wavelength range considered here for the bunch length monitors and the synchrotron radiation can be neglected compared to the edge radiation. The diffraction radiation is not imaged onto the detector and also suppressed. Thus the quantitative analysis of the system performance only regards edge radiation.
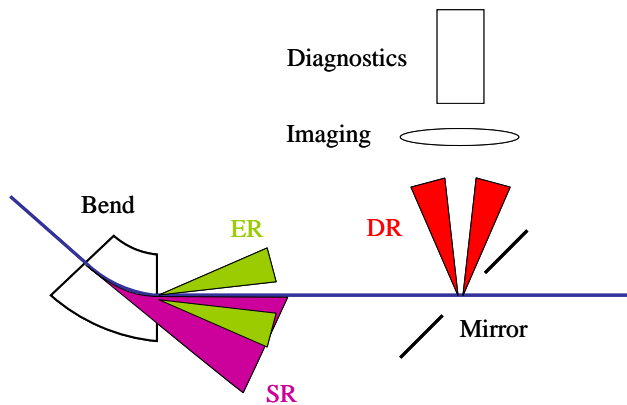

Figure 2: Schematic of the different radiation sources from a bend magnet. The synchrotron (SR) and the edge (ER) radiation are coupled into a detector with a hole mirror, which itself generates diffraction radiation (DR).

The calculation of the radiation spectrum of the edge radiation has to take into account the various apertures that the beam pipe, the in-vacuum mirror, and the imaging optics present to the radiation field. The far field radiation distribution of edge radiation equals the far field distribution of transition radiation. In the same way as transition radiation from a metal boundary can be explained as the Coulomb field of the particle acting as a radiation source at the boundary, the edge radiation can be described by a similar process where the Coulomb field is the radiation source due to the sudden change in acceleration. The transverse part of the spectral components of the Coulomb field is given by [4]

$$E\left(r,k\right) = \frac{e}{\pi v r}\frac{kr}{\gamma\beta}K_1\left(\frac{kr}{\gamma\beta}\right). \qquad (2)$$

This field is radially polarized and has a singularity on the propagation axis. The propagation of this radiation source is calculated by expressing the Coulomb field as a sum of Gauss-Laguerre modes in the Slowly Varying Envelope (SVE) approximation [5]. One linear polarization direction of the radially polarized field can be expressed with the TEM_{pl} modes with azimuthal mode number $l = 1$. The propagation through free space and focusing elements is done with the usual transformation of the complex beam parameter q. At an aperture, a new set of coefficients for the mode composition has to be calculated. The number of radial modes necessary to express the Coulomb field is $N_p = \gamma/2$ and the waist parameter is $w_0 = \sqrt{2N_p + 2}\lambda/\pi$. An approximation of the Coulomb field for 250 MeV at a wavelength of 1 mm is shown in Fig. 3. The singularity is not present in the approximation, as it represents a non-radiating field.
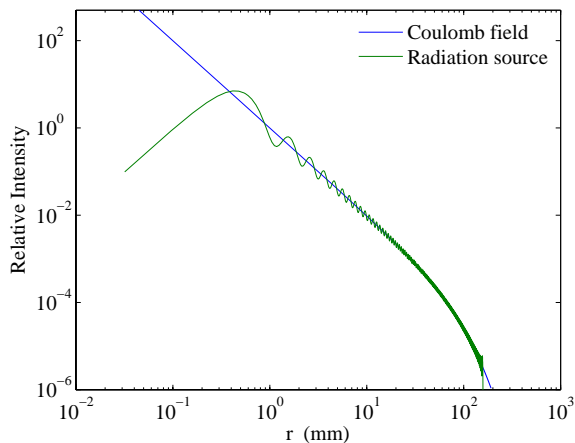

Figure 3: Coulomb field and its composition from 250 Gauss-Laguerre modes for a 250 MeV electron beam at 1 mm wavelength.

The transmission spectrum for the BC1 (see Fig. 5) and BC2 bunch length monitor (not shown) from the magnet edge to the detectors is shown in Fig. 4. The cut-off wavelength of 5 cm^{-1} (BC1) and 20 cm^{-1} (BC2) are within the relevant spectral range for both bunch length monitors.
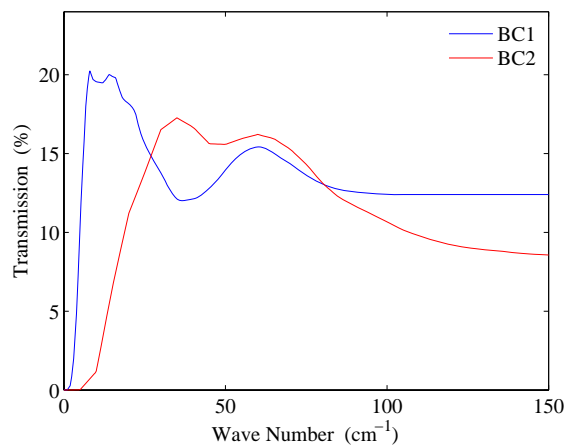

Figure 4: Simulated transmission spectrum of edge radiation in percent of the ideal far field intensity after passing through the bunch length monitor setup designed for a downstream location after bunch compressor 1 (BC1) and 2 (BC2).

BUNCH LENGTH MONITOR DESIGN

The layout for both bunch length monitors as shown in Fig. 5 for the BC1 monitor differ only in a few dimensions. For BC1, the in-vacuum mirror with a hole diameter of 15 mm is located 160 mm after the last dipole. Two 3" diameter off-axis paraboloid mirrors with a focal length of 350 mm and a beam splitter image the radiation source at the magnet edge onto the pyroelectric detectors.
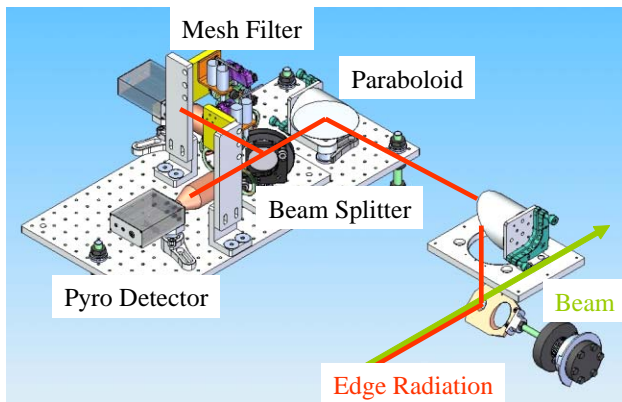

Figure 5: Drawing of the BC1 bunch length monitor. The edge radiation from the last bend magnet is reflected up with a hole mirror, collimated and re-focused with two paraboloid mirrors, and sent to two pyroelectric detectors through a beam splitter. Two sets of mesh filters can be inserted in front of the detectors.

Two sets of filters can be remotely inserted in front of the detectors. Thick grid filters [6] as high pass filters to discriminate different parts of the radiation spectrum have been developed. They consist of a stack of metal foils with
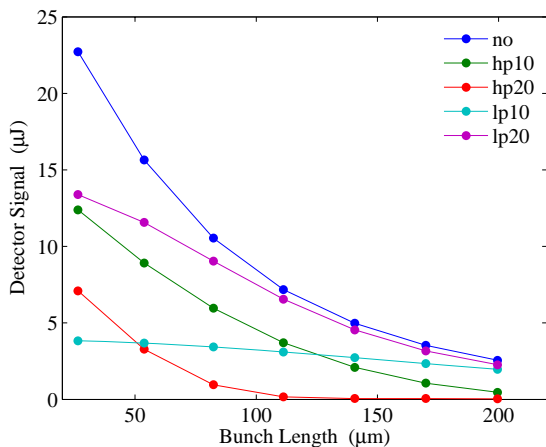

Figure 6: Bunch length sensitivity for the BC1 bunch length monitor. The detector signal represents the effectively deposited energy in a 100 μm thick LiTaO$_3$ pyroelectric detector element for different frequency filters where "lp" means low pass and "hp" high pass. The subsequent number is the cut-off wave number in cm^{-1}.

an etched hexagonal pattern of holes which act as wave guides for the mm-wave radiation. The total thickness is about twice the hole diameter D. The cut-off wavelength is given by $\lambda_c = 1.7D$. Filters for λ_c of 1000, 500, 340, and 170 μm have been realized.

The effective single bunch radiation energy as a function of bunch length for the electron beam in the 1 nC configuration is shown in Fig. 6 for the BC1 bunch length monitor. It includes the transmission through a fused quartz vacuum window, different high and low pass filters, and the absorption characteristic of a 100 μm thick metal coated LiTaO$_3$ pyroelectric detector element with 8 mm diameter. The additional black polymer coating of the actual detectors was not included, but this will only increase the performance.
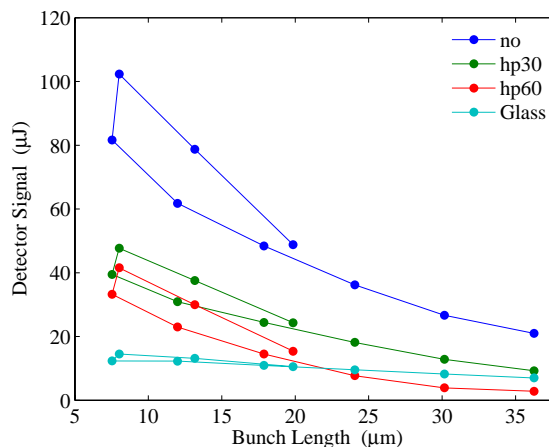

Figure 7: Bunch length sensitivity for the BC2 bunch length monitor. The "Glass" curve is for a 3 mm thick fused silica plate as low pass filter at 30 cm^{-1}.

The layout for the BC2 bunch length monitor has the hole mirror at a distance of 550 mm to allow more expansion of the narrower radiation cone due to the higher energy of 4.3 GeV. The imaging is done with a plane mirror in place of the first paraboloid and a 270 mm focal length paraboloid. The vacuum window is silicon. Fig. 7 shows the sensitivity of the bunch length monitor signal at BC2 for the 1 nC configuration. The curves show two data points for some bunch lengths for under- and over-compressed beam. The signal through the high pass filters show the different high frequency components, and combined with a low pass signal the two cases can be distinguished.

REFERENCES

[1] J. Wu et al., PAC 2005, Knoxville, May 2005, p. 1156.

[2] J. Wu et al., PAC 2005, Knoxville, May 2005, p. 428.

[3] R.A. Bosch, Rev. Sci. Instrum. 73 (2002) 1423.

[4] J.D. Jackson, "Classical Electrodynamics", 2nd ed. (Wiley, New York, 1975).

[5] H. Kogelnik and T. Li, Proc. IEEE 54 (1966) 1312.

[6] A. Roberts et al., Int. J. Infra. Mill. Waves 15 (1994) 505.